

HOT-CARRIER EFFECTS IN POLYSILICON EMITTER BIPOLAR TRANSISTORS

David Burnett and Chenming Hu

Department of Electrical Engineering and Computer Sciences
 University of California, Berkeley
 Berkeley, CA 94720
 (415)642-1010

ABSTRACT

Hot carriers are generated in self-aligned polysilicon emitter transistors under reverse bias conditions because of large electric fields which exist along the periphery of the emitter-base junction. For our devices, the degradation from constant reverse current stress can be modeled as $\Delta I_B = A Q^n$ where $n \approx 0.5$. The variation of A with the forward current at which ΔI_B is measured can be modeled as $A = B J_C^{\gamma}$ where B is independent of reverse current.

INTRODUCTION

It has been known for some time that reverse biasing the emitter-base junction can degrade the current gain of bipolar transistors [1], [2]. In advanced self-aligned transistors, the heavily doped emitter and extrinsic base regions form the junction around the periphery of the emitter and create a very large electric field. Only a few studies have considered hot-carrier effects of advanced transistors [3]-[5]. It has been observed under constant current stress conditions [3] that the degradation of β , $\Delta\beta/\beta_0$, is a linear function of Q above a critical value of Q. This work further investigates the modeling of device degradation under constant current stress for several sizes of devices and characterizes the dependence of the degradation upon the forward current at which it is measured.

EXPERIMENT

The measurements were performed on self-aligned, polysilicon emitter NPN transistors. Figure 1 illustrates the key processing steps for the transistor. The starting wafers are an n-type epitaxial layer of 0.5 Ω -cm resistivity and of 2-3 μm thickness grown on an n+ substrate. Silicon nitride is used to define the intrinsic region of the transistor in a manner similar to the process described in [6]. After the removal of the nitride, the intrinsic base implant is performed. Undoped polysilicon is deposited and then implanted with arsenic. The implant is then annealed and the arsenic driven in to form the emitter.

The constant current stress was performed by reverse biasing the emitter-base junction and applying the desired reverse current with the collector open. The forward characteristics (Gummel plot) of each device were measured before the device was stressed and then after each stress. The measurements were performed using an HP4145 semiconductor parameter analyzer. A forward current soak was observed to improve the current gain after each stress. For the devices stressed here, a forward current soak at $V_{BE} = 0.8$ V for one minute was found sufficient to saturate the current gain recovery (which was less than 15%)

after each stress and thus this soak was adopted into the measurement procedure. The stress measurements were performed on devices of three sizes, 2X4 μm^2 , 4X12 μm^2 , and 20X20 μm^2 over a range of reverse current values.

DEVICE DEGRADATION DEPENDENCE UPON REVERSE CURRENT

Figure 2(a) shows the degradation in base current for a 4X12 μm^2 device with a constant reverse current stress of 10 μA for 100 seconds. Figure 2(b) shows the current gain degradation for the same device. The degradation of β , $\Delta\beta/\beta_0$, is plotted against Q in Figure 3 for 4X12 μm^2 devices stressed at decade increments in reverse current, I_R . The measured points correspond to the same collector current density, J_C . Unlike the results in [3], $\Delta\beta/\beta_0$ for the different I_R do not fall on the same line and the individual curves are not straight lines. If, however, ΔI_B (or $\Delta \frac{1}{\beta} = I_C \Delta I_B$), is plotted as a function of Q, Figure 4, the curves are straight lines with approximately the same slope for varying I_R . This indicates that ΔI_B can be expressed as a power-law function of Q,

$$\Delta I_B = A(I_R)Q^n \quad (1)$$

where it is noted that A is a function of I_R . Using this empirical model, A and n can be extracted from the lines shown in Figure 4. For all of the devices tested and over the entire range of I_R and J_C measured, the value of n varied between .45 and .52. An average value of $n = .49$ gave a good fit to the degradation data as exemplified by the excellent fit to the $\Delta\beta/\beta_0$ points in Figure 3.

Because the value of n remains constant over the range of I_R , it is possible to then characterize the degradation at a given J_C by observing how A varies with I_R . Figure 5 shows the A versus I_R data for all three device sizes. In each case A increases with a fairly power-law dependence until it saturates at larger I_R values. One possible explanation for this phenomena is that at large values of I_R avalanche multiplication is significant enough to cause a large change in I_R for only a very small perturbation in the electric field. Because A has much less of a dependence upon the electric field than does I_R [7], A varies only slightly at large I_R . This leads to the behavior observed in Figures 3 and 4 in which the degradation curves for the largest values of I_R coincide with each other.

DEVICE DEGRADATION DEPENDENCE UPON FORWARD CURRENT

The dependence of the ΔI_B degradation upon the J_C at which ΔI_B is measured is illustrated in Figure 6 for a $4X12 \mu m^2$ device stressed at $I_R = 10 \mu A$. A value of $n = .49$ gives a good fit to the ΔI_B characteristics in Figure 6 as well as the $\Delta\beta/\beta_0$ characteristics in Figure 7. In order to characterize the device degradation over a range of J_C , the extracted values of A for various values of J_C are shown in Figure 8 for the $4X12 \mu m^2$ devices stressed at different reverse currents. This plot reveals that A exhibits a power-law dependence upon J_C and can thus be modeled as

$$A(J_C) = BJ_C^\gamma \quad (2)$$

for a device stressed at a given value of I_R . This power-law dependence of A on J_C was observed for all values of I_R for every device size.

One method of completely modeling the degradation is to determine the dependence of B and γ upon I_R . Using Equation (2), B and γ can be extracted from the lines shown in Figure 8. Figure 9 indicates that B has a weak dependence on I_R and thus B can be treated as constant. Once a value for B is determined (for a given device size), γ is chosen to provide the best fit to the A versus J_C data. Figure 10 shows the γ versus I_R characteristics for the different device sizes. At the smaller values of I_R , γ decreases as the stress current increases while at the larger I_R values γ remains fairly constant.

SUMMARY

The degradation of self-aligned, polysilicon emitter transistors is described for a wide range of constant current stress on several device sizes. The experimental results indicate that ΔI_B can be expressed as AQ^n , with $n \approx 0.5$ for our devices. Except for large values of I_R , A varies in a power-law fashion with I_R . The dependence of ΔI_B upon the forward current at which the device is operating can be expressed as $A = BJ_C^\gamma$. It is observed that n is characteristic of all devices and stress current, B is constant for a given device size, and γ varies with device size and reverse current.

ACKNOWLEDGEMENT

This research was sponsored by National Semiconductor, Lockheed, Avantek, and the University of California MICRO program.

REFERENCES

[1] D.R. Collins, "Excess current generation due to reverse bias P-N junction stress," *Applied Physics Letters*, vol. 13, pp. 264-266, October 1968.
 [2] B.A. McDonald, "Avalanche degradation of h_{FE} ," *IEEE Trans on Electron Devices*, vol. ED-17, pp. 871-878, October 1970.
 [3] S.P. Joshi, R. Lahri, and C. Lage, "Poly emitter bipolar hot carrier effects in an advanced BiCMOS technology," *Technical Digest of 1987 IEDM*, pp. 182-185, 1987.
 [4] S.A. Petersen and G.P. Li, "Hot carrier effects in advanced self-aligned bipolar transistors," *Technical Digest of 1985 IEDM*, pp. 22-25, 1985.

[5] T.C. Chen, C. Kaya, M.B. Ketchen, and T.H. Ning, "Reliability analysis of self-aligned bipolar transistor under forward active current stress," *Technical Digest of 1986 IEDM*, pp. 650-653, 1986.
 [6] G.P. Li, T.C. Chen, C.T. Chuang, J.M.C. Strok, D.D. Tang, M.B. Ketchen, and L.K. Wang, "Bipolar transistor with self-aligned lateral profile," *IEEE Electron Device Letters*, vol. EDL-8, pp. 338-340, August 1987.
 [7] D. Burnett and C. Hu, "Modeling hot-carrier effects in polysilicon emitter bipolar transistors," *IEEE Trans on Electron Devices*, submitted for publication.

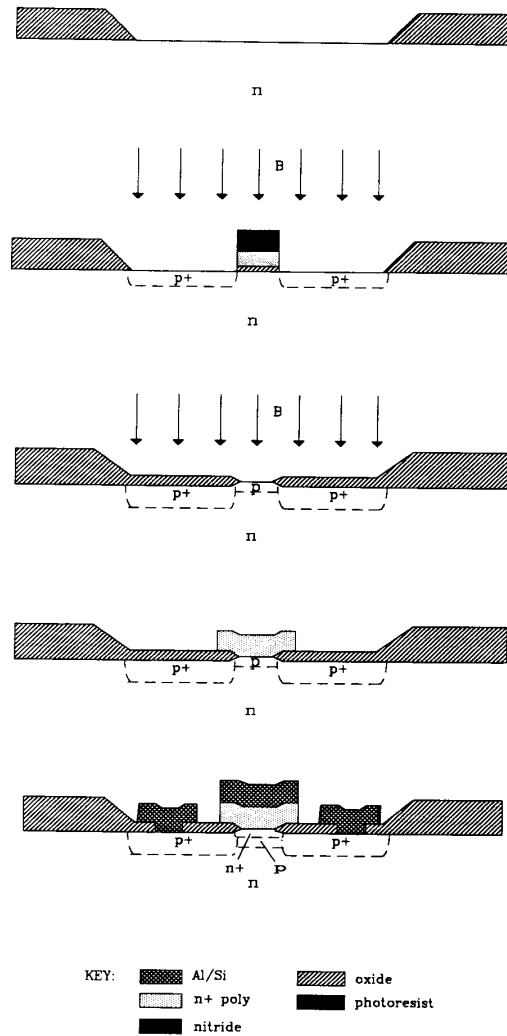


Fig.1 Key processing steps for the NPN self-aligned transistor.

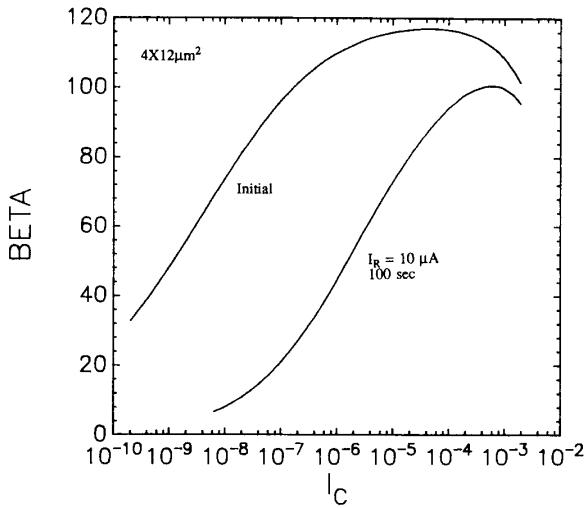
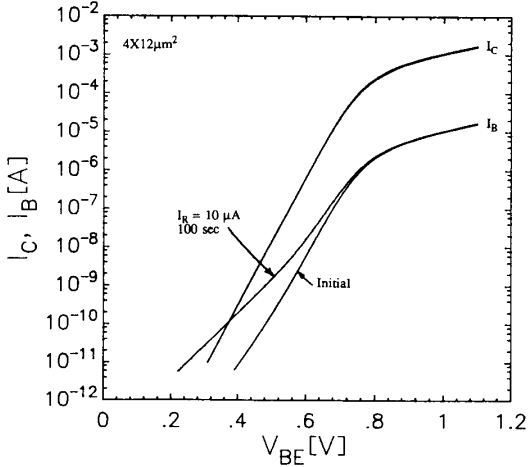


Fig.2 (a) Gummel plots showing the degradation of the base current and (b) the current gain degradation for a $4 \times 12 \mu\text{m}^2$ device stressed at $I_R = 10 \mu\text{A}$ for 100 seconds.

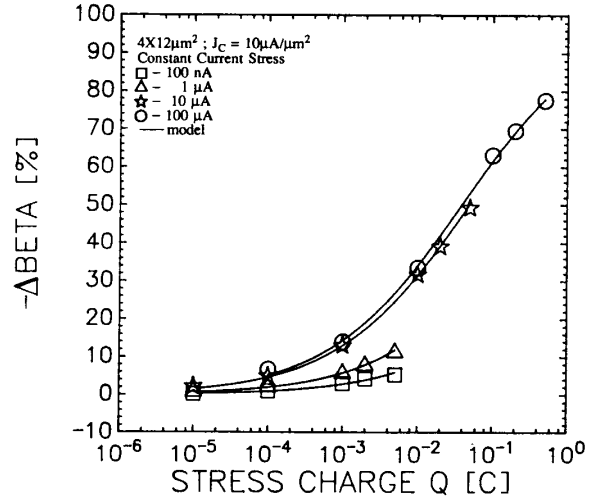


Fig.3 β degradation with constant current stress of $10 \mu\text{A}$ for a $4 \times 12 \mu\text{m}^2$ device. Values for A with $n = 0.49$ are extracted using the model of Equation (1) to generate the fit to the data points. The reverse voltages corresponding to the reverse currents are: for $I_R = 100 \text{ nA}$, $V_R = 4.2 \text{ V}$; for $I_R = 1 \mu\text{A}$, $V_R = 4.5 \text{ V}$; for $I_R = 10 \mu\text{A}$, $V_R = 5.2 \text{ V}$; for $I_R = 100 \mu\text{A}$, $V_R = 5.6 \text{ V}$.

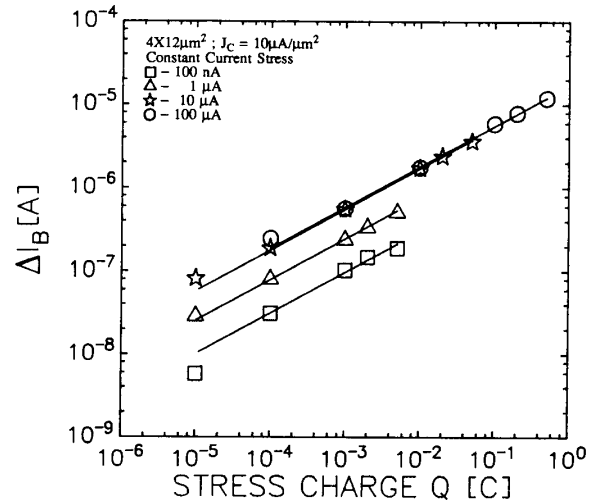


Fig.4 Degradation of ΔI_B for different stress currents. The line drawn through the points corresponds to $n = 0.49$.

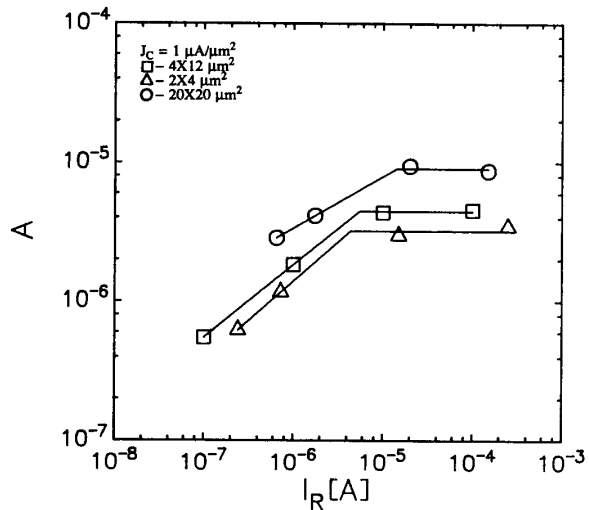


Fig. 5 Extracted values of A for three different device sizes over a range of I_R .

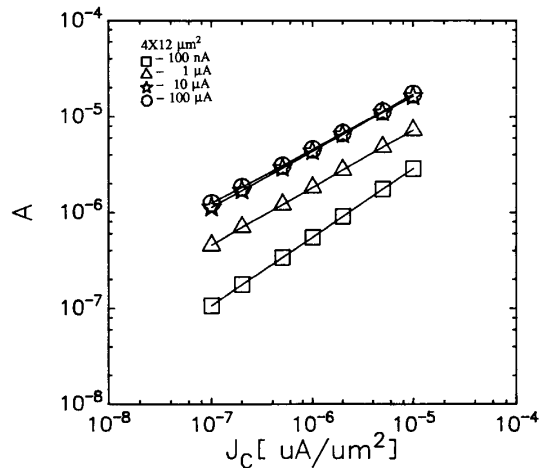


Fig. 8 Extracted values of A for different collector current densities for $4X12 \mu m^2$ devices stressed at different I_R .

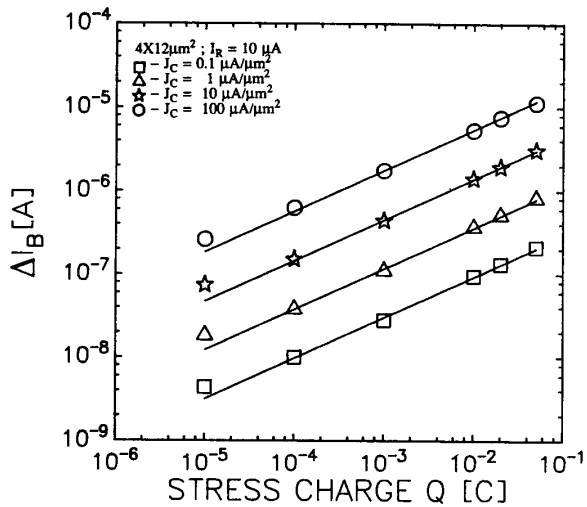


Fig. 6 Degradation of ΔI_β measured at different collector current densities for a constant current stress of $10 \mu A$.

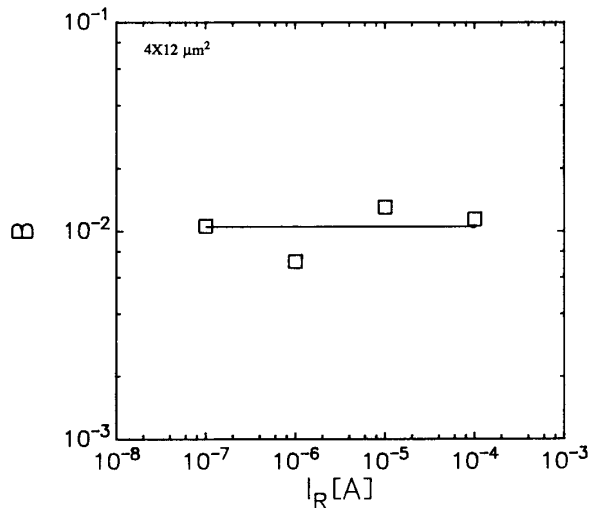


Fig. 9 Extracted values of B for different values of I_R for $4X12 \mu m^2$ devices. B is fairly independent of I_R .

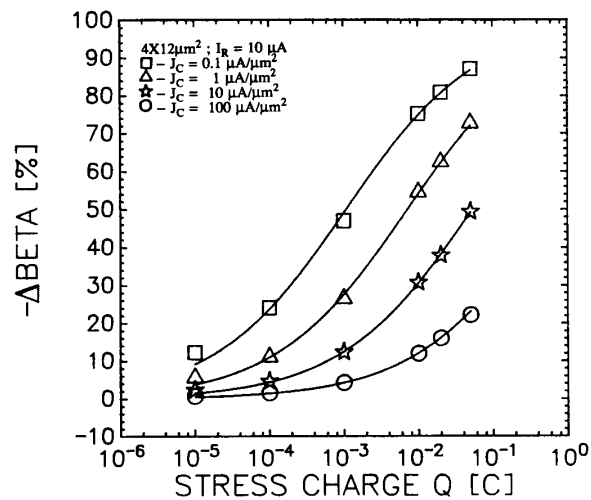


Fig. 7 β degradation measured at different collector current densities for a constant current stress of $10 \mu A$.

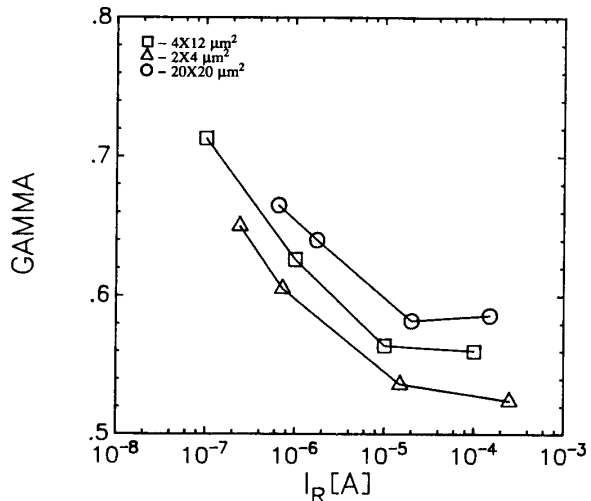


Fig. 10 Extracted values of γ using a constant value of B for each device size.